Research Square

Preprints are preliminary reports that have not undergone peer review.
They should not be considered conclusive, used to inform clinical practice,
or referenced by the media as validated information.

Metabolomics Profiling of EUS-FNA Sample Predicts Advanced Pancreatic Adenocarcinoma Prognosis

Ke Chen (chenke_1990@126.com)
Fudan University Shanghai Cancer Center https://orcid.org/0000-0002-3070-7926
Changming Zhou
Fudan University Shanghai Cancer Center
Yiping He
Fudan University Shanghai Cancer Center
Jianqiang Liu
Fudan University Shanghai Cancer Center
Xiujiang Yang
Fudan University Shanghai Cancer Center

Research

Keywords: PAC, EUS-FNA, LC-MS, WGCNA, cholesterol glucuronide

Posted Date: February 18th, 2021

DOI: https://doi.org/10.21203/rs.3.rs-200126/v1

License: This work is licensed under a Creative Commons Attribution 4.0 International License.
Read Full License

Abstract

Background

Effective anti-tumor medicine for individual cases with different prognosis risks is urgent for pancreatic adenocarcinoma (PAC) therapy. Metabolic therapy is a promising strategy for PAC. Endoscopic ultrasound-guided fine needle aspiration (EUS-FNA) is a suitable technique for the biopsy of pancreatic mass. Here, we first perform metabolome analysis with EUS-FNA samples to identify prognostic biomarkers and potential therapeutic targets in advanced PAC.

Methods

PAC underwent EUS-FNA between October 2018 to March 2019 were enrolled. The cytological sample was delivered for liquid chromatography coupled with mass spectrometry (LC-MS).

Results

A total of 60 advanced PAC with median survival of 390 days were enrolled for metabolome analysis, and 402 unique metabolites were identified. In multivariate analysis, a two-metabolite (cholesterol glucuronide and taurocholic acid 3-sulfate) risk score [hazard ratio (HR) = 1.983, 95% confidence interval (CI) = 1.362–2.887, $p < 0.001$] was constructed and proved to be independent predictors for overall survival. The C-index of the risk score was 0.64 (95% CI: 0.70–0.59). Patients in the high-risk and low-risk groups stratified by the risk score suffered different prognosis (median survival time 194 versus 480 days, $p < 0.001$). The area under the curve at 1 year was 0.685. The nomogram was depicted by combining the risk score with clinical parameters. The C-index was 0.67 (95% CI: 0.73–0.62). Finally, WGCNA identified three distinct modules and major enriched in glucose-alanine cycle and α-linolenic acid metabolism.

Conclusions

A two-metabolite risk score and nomogram with the ability to predict survival of PAC were generated. The two metabolites both showed an association with bile acid accumulation. The glucose-alanine cycle and α-linolenic acid metabolism were highly active in advanced PAC, which might be the target in future therapy.

Introduction

Pancreatic adenocarcinoma (PAC) is one of the top ten leading causes of death from cancer in the world. (1) Advanced PAC is highly lethal with median survival time less than 1 years. The traditional chemo-agents were always powerless, restricted by many factors, such as the hypo-vascularly anaerobic

microenvironment. Clinically, the urgent need for PAC therapy is an effective anti-tumor medicine for individual cases with different prognosis risks.

Metabolic process is highly active in the pancreas due to its complex exocrine and endocrine functions. Numerous studies have proved the distinctive metabolic features in the PAC anaerobic microenvironment, such as the alteration in carbon source to fuel anabolic processes, which might provide great clues in the development of metabolic therapy strategy.(2, 3)

Metabolomics is an omics technology that enables the large-scale quantification of small molecules termed metabolites. Several studies have investigated tumor metabolism in the discrimination between benign or malignant behavior and prognosis prediction in PAC. Urine, serum, or resected tissue samples with surgery were mostly applied. Among them, surgical samples were the most representative but rarest, or even unavailable, for advanced PAC. Endoscopic ultrasound-guided fine needle aspiration (EUS-FNA) is a suitable technique for the biopsy of pancreatic mass to obtain local cytological samples. Clinically, samples from EUS-FNA might be delivered to genetic sequencing to guide individual therapy.(4) In the current study, we performed metabolome analysis with EUS-FNA samples to identify prognostic biomarkers and potential therapeutic targets in advanced PAC.

Methods

Design and Patients

Previously, we conducted a retrospective study to investigate metabolomic differences between pancreatic head and body/tail cancer. Thirty PACs located in the head and 30 PACs located in the body/tail were enrolled; these samples were from patients who underwent EUS-FNA at the Department of Endoscopy, Fudan University Shanghai Cancer Center (FUSCC) between October 2018 and March 2019. With EUS-FNA, all patients were pathologically diagnosed by positive or suspicious cytology for malignancy. Survival data was collected according to FUSCC cancer patients' survival follow-up protocol. The follow-up period was measured as the date of clinical therapy to the date of the last hospital or telephone visit. All cases were allowed for a follow-up period of more than 1 year. All hospitalized patient were given informed consent about the potential sample collection when received biopsy, surgery, or et el., approved by the institutional review board of the FUSCC. Hence, need for another specific approval was waived. All cases were given informed consent about the procedure of EUS-FNA.

Sample collection and preparation

The detail of EUS-FNA procedure was described as before.(5) Two experienced endoscopists performed all the procedures with linear longitudinal ultrasound endoscopes (Pentax EG3270UK and EG-3870UTK). After inserting the needle into targeted area, a 10 ml syringe was set to activate the suction. The cytological material was rapid on-site evaluated for malignancy. When the positive diagnosis was obtained, the remain cytological samples were flushed into tubes and stored at -80 °C until use. All the materials were finally delivered to the cytological and histological examination.

The cytological sample was mixed with methanol, then vortexed for 30 s, and ultrasound for 20 min. The sample was centrifuged at 12000 rpm for 15 min. The supernatant (200 μL) was transferred to vial for Liquid chromatography coupled with mass spectrometry (LC-MS) analysis. Equal volumes (20 μL) of each sample were mixed and pooled into the quality control sample.

LC-MS analysis

All experiments were performed on an Ultimate 3000LC platform (Thermo) and equipped with Hyper gold C18 (100x2.1mm 1.9 μm) column. Chromatographic separation conditions including column temperature at 40 °C, flow rate at 0.35 mL/min, automatic injector temperature at 4 °C, injection volume at 10 μL. The mobile phase A was water plus 5 % acetonitrile and 0.1% formic acid. The mobile phase B was acetonitrile plus 0.1% formic acid. Metabolomics feature extraction and preprocessed were performed with Compound Discoverer software (Thermo). The raw data was normalized and edited into two-dimensional data matrix by excel 2010 software, including retention time, compound molecular weight, samples and peak intensity.

Survival model development

The model development and statistical analyses were performed using the R version 4.0.3. All analyses were set at two-sided p value <0.05 as the threshold for statistical significance. All metabolites were delivered into univariate Cox analysis for overall survival (OS). The candidate metabolites with P-value < 0.05 were selected for multivariate Cox analysis. The risk-score was calculated based on the identified prognostic metabolites and each coefficient. Based on mean value of risk-score, patients were stratified into high-risk and low-risk groups. Forest plots were draw to demonstrate the Hazard ratio (HR) of prognostic metabolites. The risk-score was further combined with clinical parameters to construct a integrated predictive model. Kaplan-Meier plot was depicted for different risk groups. To cluster the metabolites, the Weighted Gene Co-expression Network Analysis (WGCNA) was performed with the R package. In the sample clustering, one outlier was identified and excluded. A soft threshold of 3 was set, based on the scale free topology model. In the module clustering, the minimal metabolite number was set as 50. The enrichment analysis was performed in online website MetaboAnalyst.(6)

Results

The clinical features of all 60 PACs were described in Table 1. The mean age was 64.6 years, and 38 cases were male. The lesions were located in the pancreatic head in 30 cases and body/tail in 30 cases. The mean size was 36.0 mm (range, 21.0–60.5 mm). Clinically, 48 (80.0%) cases received gemcitabine-based chemotherapy, 2 cases received mFOLFIRINOX, and the remaining 10 cases did not receive any chemotherapy.

Table 1
Clinical features of included PAC.

Age (years, mean ± SD)	**64.6 ± 9.1**
Gender (n, %)	
Female	22 (36.7%)
Male	38 (63.3%)
BMI (mean ± SD)	22.3 ± 2.8
Location (n, %)	
Head	30 (50.0%)
Body/tail	30 (50.0%)
Lesion size (mm, mean ± SD)	36.0 ± 8.7
Dilation of Bile duct (n, %)	
Negative	48 (80.0%)
Positive	12 (20.0%)
Dilation of Pancreatic duct (n, %)	
Negative	24 (40.0%)
Positive	36 (60.0%)
Serum Liver test	
Albumin (g/L, mean ± SD)	42.3 ± 4.3
Blood urea nitrogen (μmol/L, mean ± SD)	4.8 ± 1.3
Lactic dehydrogenase (U/L, mean ± SD)	172.3 ± 58.2
Fasting blood glucose (mmol/L, mean ± SD)	6.6 ± 2.7
Uric acid (μmol/L, mean ± SD)	267.8 ± 73.3
Serum CA199 (n, %)	
Normal	9 (15.0%)
Elevation	51 (85.0%)
Therapy (n, %)	
Gemcitabine-based chemo	48 (80.0%)
mFOLFIRINOX	2 (3.3%)
Other	10 (16.7%)

In LC-MS analysis, 2,550 features and 2,307 features were obtained at the electrospray ionization negative and positive (ESI^- and ESI^+) ionic modes. A total of 587 metabolites were identified and annotated based on compound molecular weight and peak intensity. For metabolites with multiple items, the average level was calculated, and 402 unique metabolites were finally included in the analysis.

Collectively, all patients with PAC were followed up for at least 1 year. The median follow-up time was 352 days, ranging from 0 day to 762 days. Forty-five patients died at the time of the last follow-up (January 15, 2021), which included all the ten cases without any chemotherapy. The median survival time was 390 days, ranging from 324 days to 492 days. Initially, 16 metabolites were identified by univariate analysis (Fig. 1). Further multivariate analysis indicated that cholesterol glucuronide (HR = 1.181, 95%CI = 1.092–1.276, $p < 0.001$) and taurocholic acid 3-sulfate (HR = 1.132, 95%CI = 1.058–1.210, $p < 0.001$) were the independent predictors for overall survival (OS). As shown in the human metabolome database, both cholesterol glucuronide and taurocholic acid 3-sulfate were associated with bile acid metabolism. In PAC, the head tumor always induced the obstructive dilation of the bile duct and cholestasis instead of the body/tail tumor. As shown in **Supplemental Fig. 1**, the level of taurocholic acid 3-sulfate was slightly higher in cancers with head location and bile duct dilation, than body/tail location and bile duct non-dilation. As for cholesterol glucuronide, no any significant difference in such two conditions.

In accordance with the coefficient of prognostic metabolites, the risk score was calculated and stratified into the high-risk (n = 15) and low-risk (n = 45) groups. The C-index of the risk score was 0.64 (95% CI: 0.70–0.59). The areas under the curve at 1 and 2 years were 0.685 and 0.588, respectively (Fig. 2A). As shown in Fig. 2B, the levels of the two metabolites were higher in the high-risk group than in the low-risk group ($p < 0.001$ for cholesterol glucuronide, $p < 0.05$ for taurocholic acid 3-sulfate). The Kaplan–Meier plot indicated that the high-risk group had significantly worse prognosis than the low-risk group ($p < 0.001$), with median survival times of 195 and 480 days, respectively (Fig. 2C).

Further, clinical parameters were incorporated into the Cox model with risk score to construct the predictive model. With univariate and multivariate analyses, therapy (HR = 0.270, 95% CI = 0.097–0.747, $p = 0.012$; Fig. 3) and risk score (HR = 1.983, 95% CI = 1.362–2.887, $p < 0.001$; Fig. 3) were found to be the independent predictors for prognosis. The predictive model was depicted in the nomogram (Fig. 4), with a C-index of 0.67 (95% CI: 0.73–0.62). A credible predictive model based on the metabolites was finally constructed for PAC prognosis.

Subsequently, we attempted to investigate the metabolic profile in different risk groups. As shown in the volcano plot (Fig. 5A), 29 metabolites showed higher levels in the high-risk group than in the low-risk group, and the difference was statistically significant ($p < 0.05$). The detailed level of significant metabolites is shown in the heatmap (Fig. 5B).

Finally, we performed WGCNA to cluster the metabolites and identified three distinct modules, namely, turquoise, blue, and grey (Figs. 6A and 6B). All the three showed no significant association with clinical parameters (**Supplemental Fig. 2**). A total of 243 metabolites were clustered into the turquoise module

and majorly enriched in the glucose-alanine cycle. A total of 150 metabolites were clustered into the blue module and majorly enriched in α-linolenic acid metabolism. Only nine metabolites were clustered into the grey module, and enriched in no metabolic pathway. Details are shown in Figs. 6C and 6D.

Discussion

The current study validated the ability of metabolomics profile by using EUS-FNA-acquired cytological samples in the prediction of PAC prognosis. A two-metabolite risk score (cholesterol glucuronide and taurocholic acid 3-sulfate) predicted the OS. We further depicted a nomogram by combining the risk score and clinical parameters. Finally, WCGNA clustered all metabolites into three modules, which majorly enriched into the glucose-alanine cycle and α-linolenic acid metabolism.

Several studies investigated tumor metabolism in the prognosis prediction of PAC through the use of urine, serum, or surgical samples. Battini *et al.* indicated that surgical sample-based metabolic biomarkers can predict the long-term survival of resectable PAC.(7) Thereafter, serum samples were also proved to be useful in the prediction of recurrence-free survival.(8) However, the reliability of urine and serum samples may be questioned because they are susceptible to several factors, including gender, age, body mass, and metabolic diseases.(9–11) Surgical samples are suitable and representative but infeasible for most advanced pancreatic cancer. EUS-FNA is a suitable technique for the biopsy of pancreatic mass to obtain local cytological samples. Clinically, samples from EUS-FNA might also be delivered to genetic sequencing to guide individual therapy.(4) However, the application of EUS-FNA in metabolomics has never been reported. In Shanghai Cancer Center, we established a metabolomics analysis system with EUS-FNA-acquired cytological samples, which proved to be reliable. Here, we initially validate the predictive value for advanced PAC prognosis with this system.

In the 402 identified unique metabolites, only cholesterol glucuronide and taurocholic acid 3-sulfate were proved to be independent predictors for OS. Glucuronidation is a pathway for the detoxification and elimination of toxic substances. Cholesterol glucuronide is generated in the liver by UDP glucuronyltransferase, and it is reported to prevent cholesterol gallstone initiation via bilirubin biotransformation.(12) Bile acid sulfation is a minor pathway in normal circumstances but increases in the presence of cholestasis to accelerate renal clearance and decrease intestinal reabsorption. Physically, both the two metabolites are involved in the feedback control of bile acid accumulation. Experiments already revealed the toxicity of bile acid on pancreatic acinar cell and ductal epithelium.(13, 14) In our data, both metabolites significantly increased in the high-risk group and independently predicted PAC prognosis. We speculated that elevation of the two metabolites was a protective consequence of cholestasis induced by PAC progression. The predictive value of bile duct dilation was also evidence of such a conjecture. However, one point should be noted. PAC in the head results in bile duct dilation and cholestasis, but PAC in body/tail presents negative bile duct dilation and suffers no direct stimulation from bile acid. Our data did not show quite significant difference of both two metabolites as for tumor location and bile duct dilation. We speculated that bile acid might suffer from stacked excretion in all locations and is exerted on PAC cells via systemic circulation.

The WGCNA found that all the metabolites could be clustered into three distinct modules, and they were enriched in glucose-alanine cycle or α-linolenic acid metabolism. Cancer shows different metabolic features, compared with normal counterparts, such as the alteration in carbon source to fuel anabolic processes.(15) Alanine, a non-essential amino acid, was reported to be secreted by pancreatic stellate cell and outcompeted glucose-derived carbon in PAC to fuel the tricarboxylic acid cycle.(16) The current data verified that the glucose-alanine cycle was highly active in PAC, which indicate its may be potential target for future anti-cancer therapy. Studies already proved the protective effect of α-linolenic acid in several inflammatory conditions, such as ulcerative colitis and hepatic steatosis.(17, 18) Meanwhile, epidemiologic evidence on the risk of PAC remains controversial.(19) As a member of n-3 polyunsaturated fatty acids, α-linolenic acid plays a distinctive role of carbon source substitution in athletes' aerobic performance when the carbohydrate reserve is consumed.(20) In advanced PAC, whether α-linolenic acid contributes to the carbon source into anaerobic metabolism still needs further investigation.

Our work had several limitations. First, the primary target of the cohort was metabolic profile in different PAC locations. Thus, head and body/tail PAC with even numbers were enrolled. Such a condition might generate selection bias to the current analysis, to some extent. Second, the current predictive model should be validated in further external cohorts.

In conclusion, our data validated the ability of metabolic profiles by using EUS-FNA-acquired cytological samples in the prediction of PAC prognosis. A risk score formulated by cholesterol glucuronide and taurocholic acid 3-sulfate, which both were associated with bile acid accumulation, was constructed. Furthermore, a nomogram was depicted to predict the survival probability for advanced PAC. Enrichment analysis indicated that glucose-alanine cycle and α-linolenic acid metabolism demonstrated high activity in advanced PAC, which might be a potential target in future therapy.

Declarations

Ethics approval and consent to participate

All hospitalized patient were given informed consent about the potential sample collection when received biopsy, surgery, or et el., approved by the institutional review board of the Fudan University Shanghai Cancer Center. Hence, need for another specific approval was waived. All cases were given informed consent about the procedure of EUS-FNA.

Consent for publication

Not applicable.

Availability of data and materials

The datasets used and/or analyzed during the current study are available from the corresponding author on reasonable request.

Competing interests

The authors declare that they have no competing interests.

Funding

This work was supported by the grant from the Program of Shanghai Anti-cancer Association (No. SHCY-JC-201931).

Authors' contributions

CK designed and supervised the project. YXJ and CK performed the clinical procedure. CK, ZCM, and HYP collected the samples and performed the analysis and interpreted data. CK and LJQ drafted the manuscript. YXJ revised the manuscript for important content.

Acknowledgements

Not applicable.

References

1. Karakas Y, Lacin S, Yalcin S. Recent advances in the management of pancreatic adenocarcinoma. Expert review of anticancer therapy. 2018;18(1):51-62.
2. Vaziri-Gohar A, Zarei M, Brody JR, Winter JM. Metabolic Dependencies in Pancreatic Cancer. Frontiers in oncology. 2018;8:617.
3. Mayers JR, Torrence ME, Danai LV, Papagiannakopoulos T, Davidson SM, Bauer MR, et al. Tissue of origin dictates branched-chain amino acid metabolism in mutant Kras-driven cancers. Science. 2016;353(6304):1161-5.
4. Wang X, Gao J, Ren Y, Gu J, Du Y, Chen J, et al. Detection of KRAS gene mutations in endoscopic ultrasound-guided fine-needle aspiration biopsy for improving pancreatic cancer diagnosis. The American journal of gastroenterology. 2011;106(12):2104-11.
5. Liu Y, Chen K, Yang XJ. Endoscopic ultrasound-guided fine-needle aspiration used in diagnosing gastric linitis plastica: Metastatic lymph nodes can be valuable targets. Journal of gastroenterology and hepatology. 2019;34(1):202-6.
6. Chong J, Soufan O, Li C, Caraus I, Li S, Bourque G, et al. MetaboAnalyst 4.0: towards more transparent and integrative metabolomics analysis. Nucleic acids research. 2018;46(W1):W486-W94.
7. Battini S, Faitot F, Imperiale A, Cicek AE, Heimburger C, Averous G, et al. Metabolomics approaches in pancreatic adenocarcinoma: tumor metabolism profiling predicts clinical outcome of patients. BMC Medicine. 2017;15(1).
8. Rho SY, Lee S-G, Park M, Lee J, Lee SH, Hwang HK, et al. Developing a preoperative serum metabolome-based recurrence-predicting nomogram for patients with resected pancreatic ductal

adenocarcinoma. Scientific Reports. 2019;9(1).

9. Trabado S, Al-Salameh A, Croixmarie V, Masson P, Corruble E, Feve B, et al. The human plasma-metabolome: Reference values in 800 French healthy volunteers; impact of cholesterol, gender and age. PloS one. 2017;12(3):e0173615.
10. Darst BF, Koscik RL, Hogan KJ, Johnson SC, Engelman CD. Longitudinal plasma metabolomics of aging and sex. Aging. 2019;11(4):1262-82.
11. Cirulli ET, Guo L, Leon Swisher C, Shah N, Huang L, Napier LA, et al. Profound Perturbation of the Metabolome in Obesity Is Associated with Health Risk. Cell metabolism. 2019;29(2):488-500 e2.
12. Duvaldestin P, Mahu JL, Metreau JM, Arondel J, Preaux AM, Berthelot P. Possible role of a defect in hepatic bilirubin glucuronidation in the initiation of cholesterol gallstones. Gut. 1980;21(8):650-5.
13. Perides G, Laukkarinen JM, Vassileva G, Steer ML. Biliary acute pancreatitis in mice is mediated by the G-protein-coupled cell surface bile acid receptor Gpbar1. Gastroenterology. 2010;138(2):715-25.
14. Joshi S, Cruz E, Rachagani S, Guha S, Brand RE, Ponnusamy MP, et al. Bile acids-mediated overexpression of MUC4 via FAK-dependent c-Jun activation in pancreatic cancer. Molecular oncology. 2016;10(7):1063-77.
15. Son J, Lyssiotis CA, Ying H, Wang X, Hua S, Ligorio M, et al. Glutamine supports pancreatic cancer growth through a KRAS-regulated metabolic pathway. Nature. 2013;496(7443):101-5.
16. Sousa CM, Biancur DE, Wang X, Halbrook CJ, Sherman MH, Zhang L, et al. Pancreatic stellate cells support tumour metabolism through autophagic alanine secretion. Nature. 2016;536(7617):479-83.
17. Bae SJ, Kim JE, Choi HJ, Choi YJ, Lee SJ, Gong JE, et al. alpha-Linolenic Acid-Enriched Cold-Pressed Perilla Oil Suppress High-Fat Diet-Induced Hepatic Steatosis through Amelioration of the ER Stress-Mediated Autophagy. Molecules. 2020;25(11).
18. Kim J, Ahn M, Choi Y, Kang T, Lee NH, Kim GO, et al. Alpha-Linolenic Acid Alleviates Dextran Sulfate Sodium-Induced Ulcerative Colitis in Mice. Inflammation. 2020;43(5):1876-83.
19. Gong Z, Holly EA, Wang F, Chan JM, Bracci PM. Intake of fatty acids and antioxidants and pancreatic cancer in a large population-based case-control study in the San Francisco Bay Area. International journal of cancer. 2010;127(8):1893-904.
20. Lyudinina AY, Bushmanova EA, Varlamova NG, Bojko ER. Dietary and plasma blood alpha-linolenic acid as modulators of fat oxidation and predictors of aerobic performance. Journal of the International Society of Sports Nutrition. 2020;17(1):57.

Figures

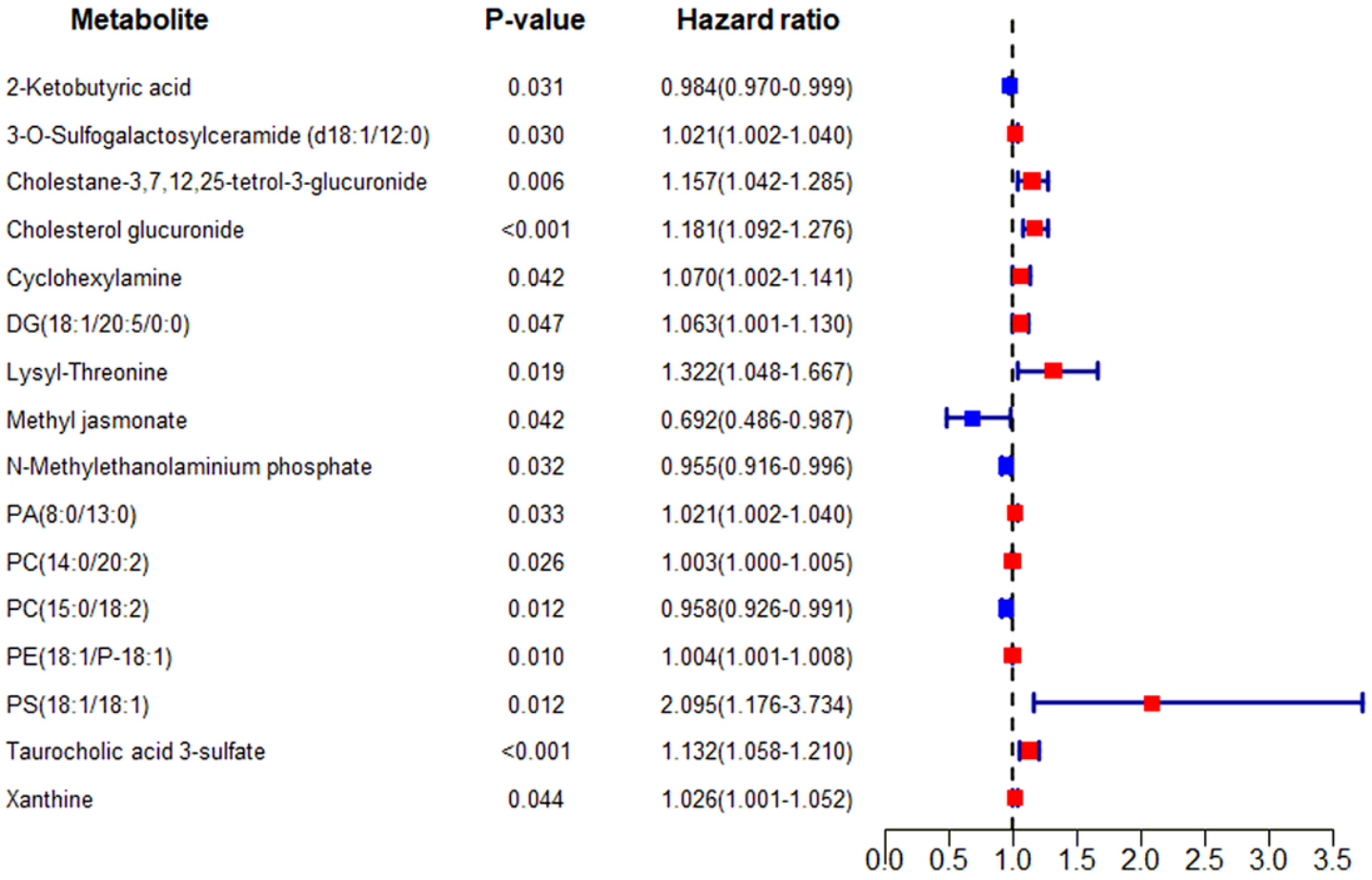

Figure 1

Identification of the prognosis-associated metabolites for PAC. In the forest plot, 16 metabolites were identified by univariate analysis. Multivariate analysis indicated that cholesterol glucuronide and taurocholic acid 3-sulfate were the independent predictors for OS.

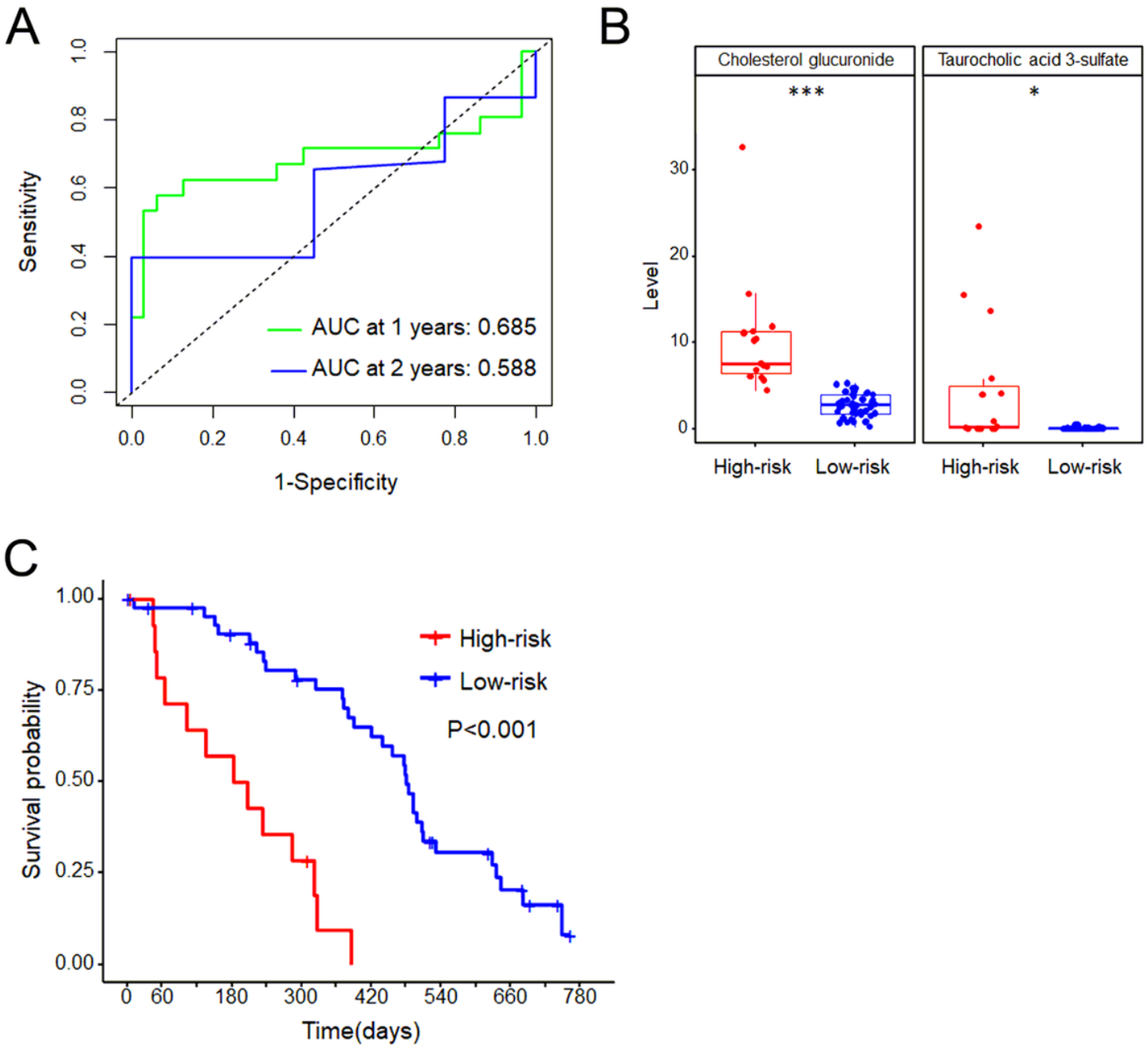

Figure 2

Prognostic analysis of the two metabolites' risk score. The AUC at 1 and 2 years were 0.685 and 0.588, respectively (A). Level of the two metabolites in the high-risk and low-risk group were shown (B). Kaplan–Meier plots showed PAC OS between the high-risk group and low-risk group (C).

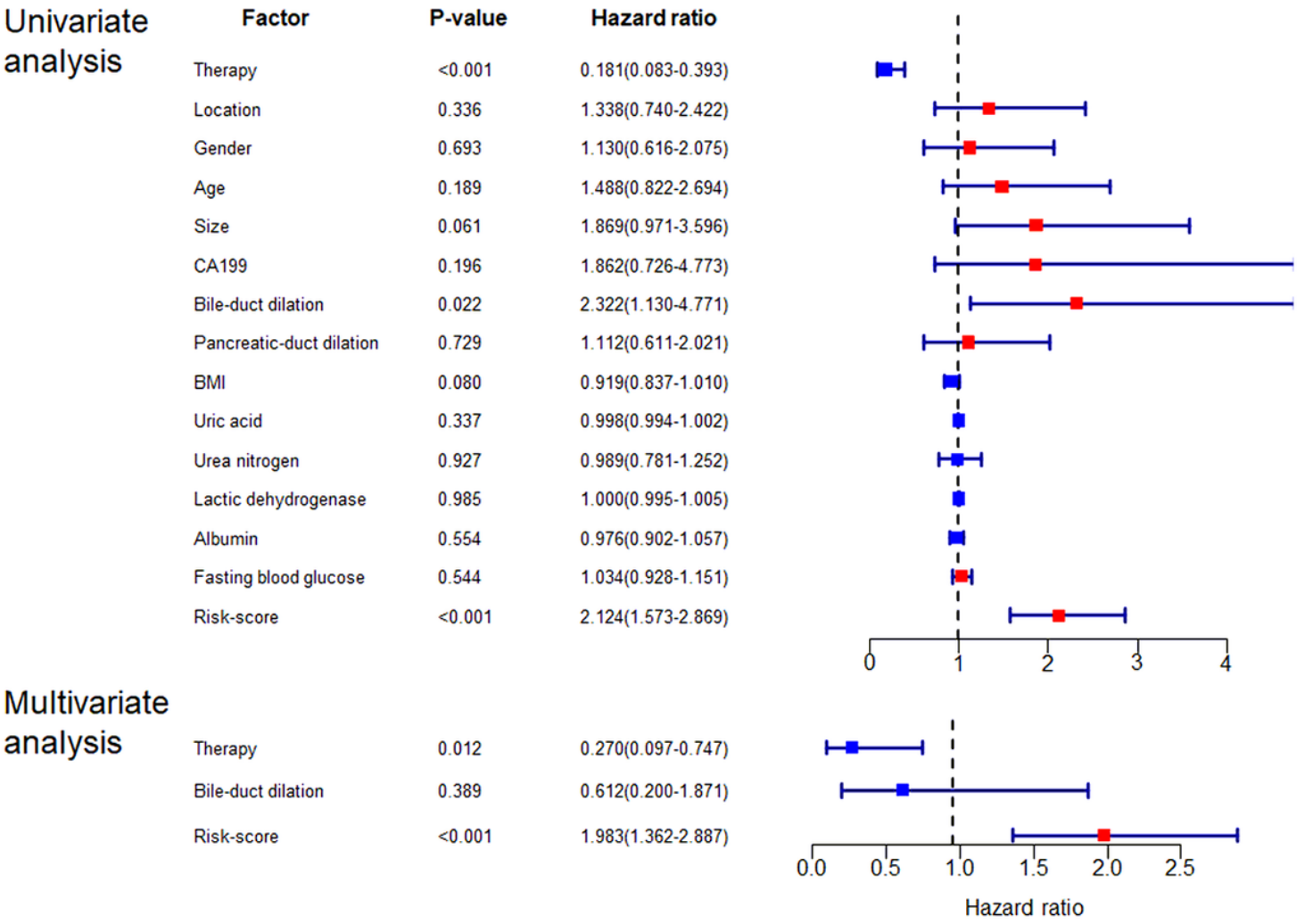

Figure 3

Identification of the metabolites and clinical associated predictors for PAC survival. With the univariate and multivariate analyses, therapy and risk score were the independent predictors for prognosis.

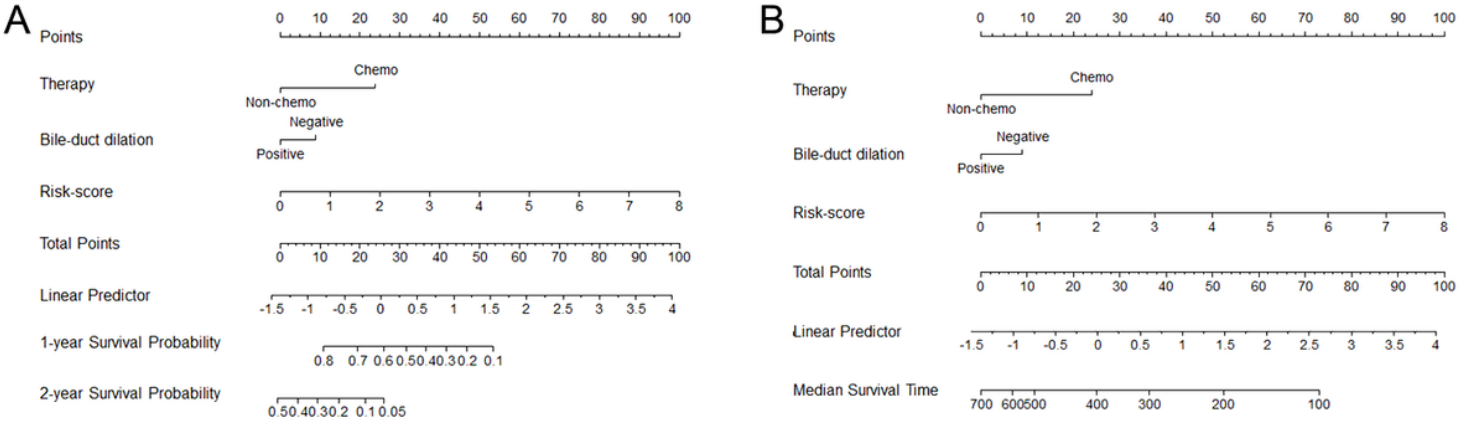

Figure 4

Nomogram of the predictive model for PAC prognosis. The survival probability is shown in A, and median survival time is shown in B.

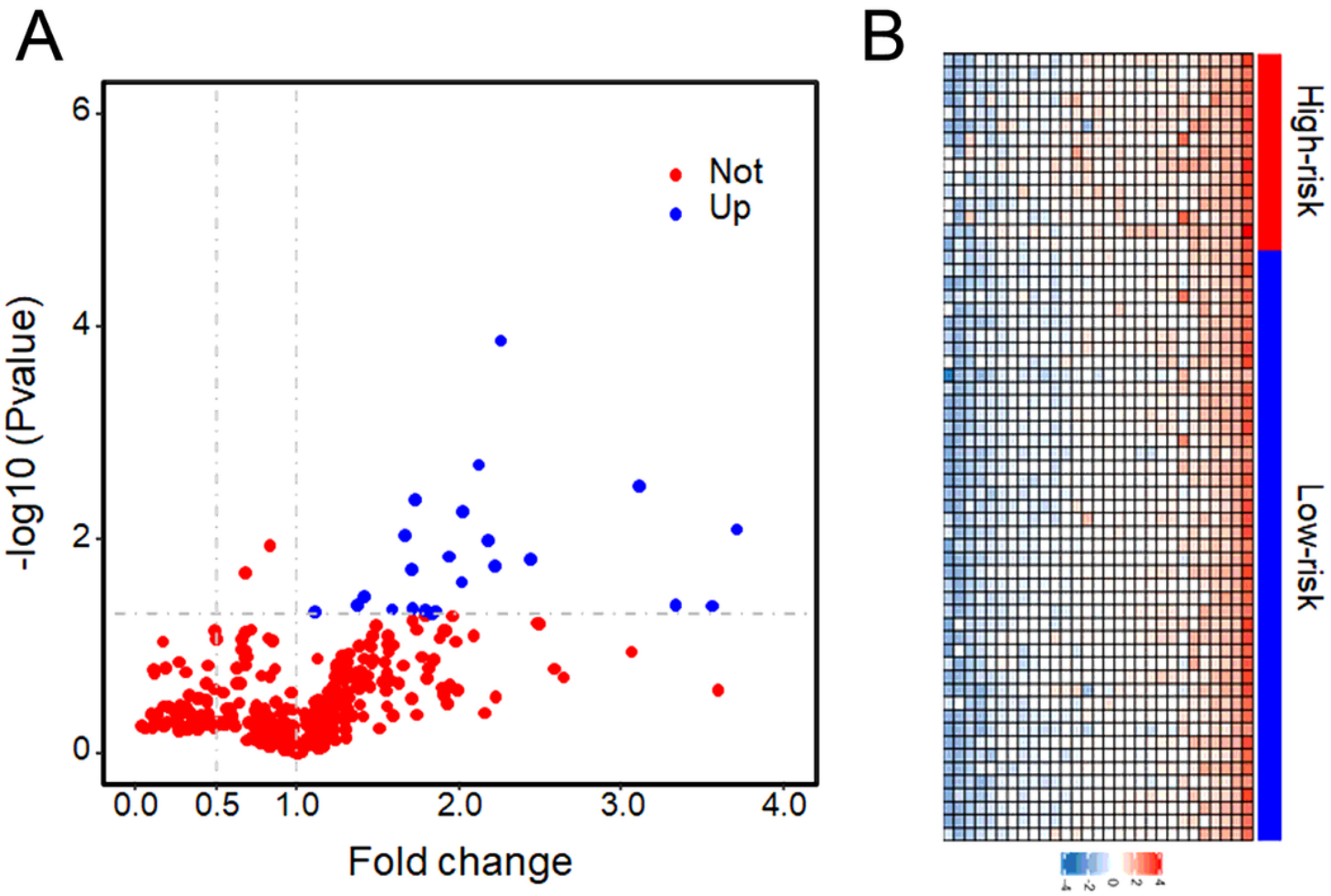

Figure 5

Level of metabolites in different risk groups. As shown in the volcano plot (A), 29 metabolites showed higher levels in the high-risk group than in the low-risk group, with the difference being statistically significant ($p<0.05$). The dashed line indicates the significant threshold p-value of 0.05 and absolute value of fold change of 1. The detailed level of significant metabolites is shown in the heatmap (B).

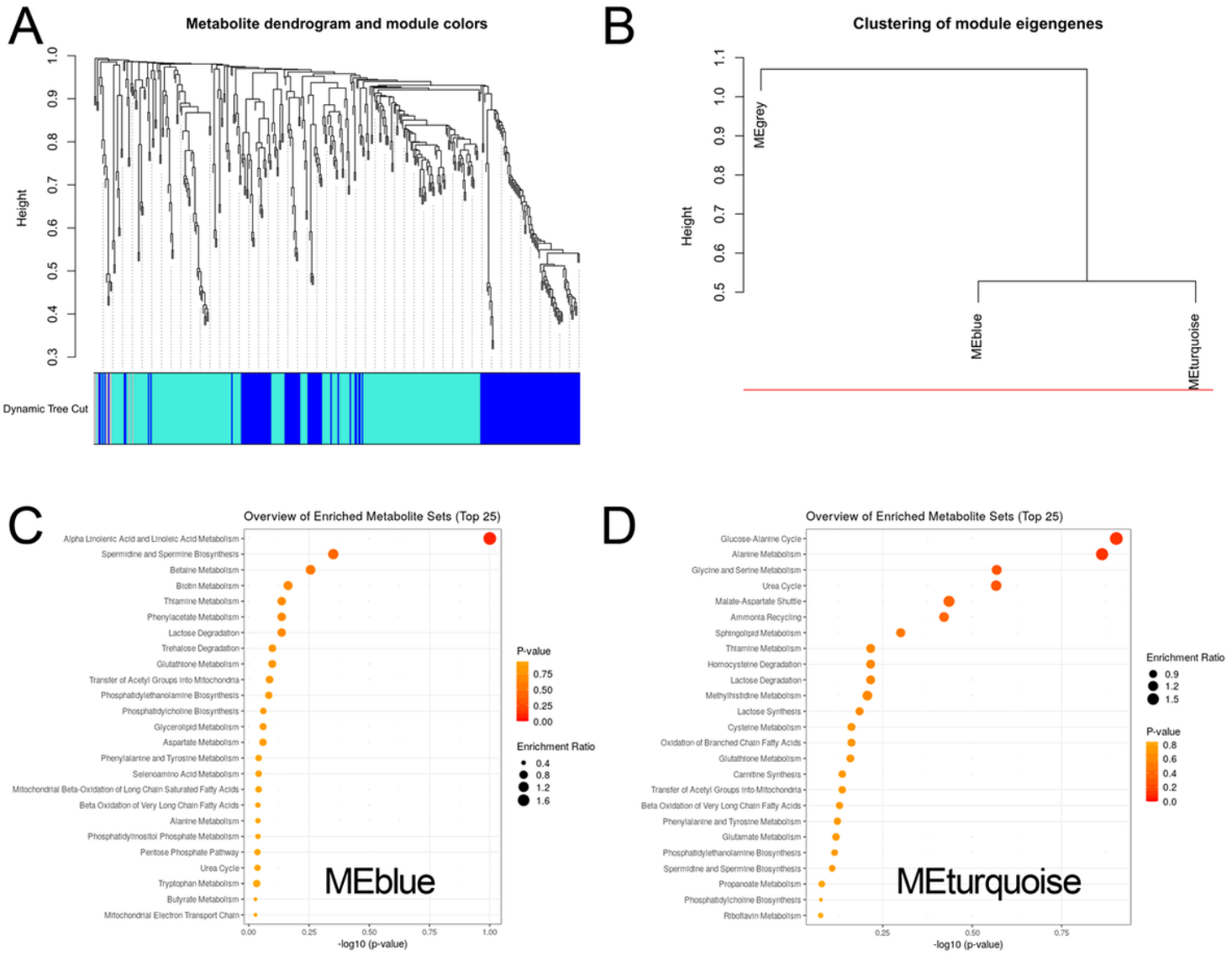

Figure 6

WGCNA for clustering and enrichment. As shown in the dendrogram (A, B), all metabolites were clustered into three distinct modules, namely, turquoise, blue, and grey. The bubble plot indicated that metabolites in the blue module were majorly enriched in α-linolenic acid metabolism (C), and metabolites in the turquoise module were majorly enriched in glucose-alanine cycle (D).

Supplementary Files

This is a list of supplementary files associated with this preprint. Click to download.

- supplementalFigure1.tif
- supplementalFigure2.tif